IBRO Reports 5 (2018) 43–53

Contents lists available at ScienceDirect

IBRO Reports

journal homepage: www.elsevier.com/locate/ibror

Research Paper

Neurodegeneration in the olfactory bulb and olfactory deficits in the *Ccdc66* -/- mouse model for retinal degeneration

Sabrina Schreiber[a], Elisabeth Petrasch-Parwez[b], Elke Porrmann-Kelterbaum[a], Eckart Förster[b], Jörg T. Epplen[a,c], Wanda M. Gerding[a,*]

[a] Department of Human Genetics, Ruhr-University, 44780 Bochum, Germany
[b] Department of Neuroanatomy and Molecular Brain Research, Ruhr-University, 44780 Bochum, Germany
[c] Department of Biochemistry and Molecular Medicine, University of Witten-Herdecke, ZBAF, 58453 Witten, Germany

ARTICLE INFO

Keywords:
Ccdc66
Mouse model
Olfactory bulb
Neurodegeneration
Retinitis pigmentosa

ABSTRACT

The *Ccdc66*-deficient (*Ccdc66* -/-) mouse model exhibits slow progressive retinal degeneration. It is unclear whether CCDC66 protein also plays a role in the wildtype (WT; *Ccdc66* +/+) mouse brain and whether the lack of *Ccdc66* gene expression in the *Ccdc66* -/- mouse brain may result in morphological and behavioral alterations.

CCDC66 protein expression in different brain regions of the adult WT mouse and in whole brain during postnatal development was quantified by SDS-PAGE and Western blot. *Ccdc66* reporter gene expression was visualized by X-gal staining. Selected brain regions were further analyzed by light and electron microscopy. In order to correlate anatomical with behavioral data, an olfactory habituation/dishabituation test was performed.

CCDC66 protein was expressed throughout the early postnatal development in the WT mouse brain. In adult mice, the main olfactory bulb exhibited high CCDC66 protein levels comparable to the expression in the retina. Additionally, the *Ccdc66* -/- mouse brain showed robust *Ccdc66* reporter gene expression especially in adult olfactory bulb glomeruli, the olfactory nerve layer and the olfactory epithelium. Degeneration was detected in the *Ccdc66* -/- olfactory bulb glomeruli at advanced age. This degeneration was also reflected in behavioral alterations; compared to the WT, *Ccdc66* -/- mice spent significantly less time sniffing at the initial presentation of unknown, neutral odors and barely responded to social odors.

Ccdc66 -/- mice develop substantial olfactory nerve fiber degeneration and alteration of olfaction-related behavior at advanced age. Thus, the *Ccdc66* -/- mouse model for retinal degeneration adds the possibility to study mechanisms of central nervous system degeneration.

Introduction

Retinitis pigmentosa (RP) constitutes a group of inherited diseases that cause retinal degeneration and a consequent loss of vision in humans. The main characteristic of the classic type of RP is the progressive degeneration of the photoreceptor cells and/or the adjacent retinal pigment epithelium (Dias et al., 2017). More than 250 genes have been associated with retinal diseases [RetNet™Retinal Information Network; available at https://sph.uth.edu/retnet/], and the inheritance mode is heterogeneous (including autosomal-dominant and autosomal-recessive, X-chromosomal, *etc.*; Dryja et al., 1990; Rosenfeld et al., 1992; Schwahn et al., 1998; Dias et al., 2017). Besides affecting the retina, up to 20–30% of the RP cases appear as part of a multi-systemic disease, for example accompanied by kidney abnormalities, reduced gonadal function in Bardet-Biedl syndrome or hearing difficulties in Usher syndrome (Yan and Liu, 2010; Mockel et al., 2011). Therefore, animal models are of pioneering relevance to identify implicated genes and their respective disease-causing mutations in humans. These mutations in animal models are also useful for determining the underlying biochemical and pathological mechanisms as well as for describing phenotype characteristics. The broad variety of animal, especially mouse models of retinal degeneration mirrors the heterogeneity of progression

Abbreviations: AG, astroglia; *Ccdc66* -/-, *Ccdc66*-deficient; *Ccdc66* +/+, WT, wildtype; CTX, cortex; De, dendrite; EPL, external plexiform layer; GAPDH, glyceraldehyde-3-phosphate dehydrogenase; GL, glomerular layer; gPRA, generalized progressive retinal atrophy; ioD, integrated optic density; IPL, internal plexiform layer; m, month/s; M, mitochondrion; ML, mitral cell layer; MOB, main olfactory bulb; OE, olfactory epithelium; ONF, olfactory nerve fibers; ONL, olfactory nerve layer; ORN, olfactory receptor neuron(s); P, postnatal day; PBS, phosphate-buffered saline; PG, periglomerular cells; RIPA, radioimmunoprecipitation assay; RMS, rostral migratory stream; RP, retinitis pigmentosa; SC, supporting cell; SEZ, subependymal zone; SVZ, subventricular zone

* Corresponding author at: Department of Human Genetics, MA 5/135, Ruhr-University, Universitätsstrasse 150, 44801 Bochum, Germany.
E-mail address: wanda.gerding@rub.de (W.M. Gerding).

https://doi.org/10.1016/j.ibror.2018.08.004
Received 10 April 2018; Accepted 23 August 2018

and severity of human retinal degeneration, with a spectrum that ranges from fast degeneration to a human RP-like slow progressive decline of retinal function (Dalke and Graw, 2005; Baehr and Frederick, 2009).

In order to study retinal degeneration, and more specifically RP, the *Coiled-Coil Domain Containing 66* - deficient (*Ccdc66* -/-) mouse, engineered by a 5′ gene-trap-mediated disruption of the *Ccdc66* gene (5′of mouse exon 4; accession no. NM_177111), was presented as a model of human RP-like, autosomal recessively inherited retinal degeneration (Gerding et al., 2011). The model was generated based on the identification of the causative *CCDC66*-mutation in autosomal recessive generalized progressive retinal atrophy (gPRA) in Schapendoes dogs (Dekomien et al., 2010). The *Ccdc66* -/- mouse lacks intact full-length *Ccdc66* RNA and CCDC66 protein, which results in first signs of degeneration of retinal photoreceptors around postnatal day 13. Retinal degeneration progresses slowly by thinning mainly of the outer retina to half of the normal thickness around the age of six months. Functional retinal impairment has also been observed by electroretinography measurements showing gradually reduced scotopic a-wave (primary rod-driven) and photopic b-wave (primary cone-driven) amplitudes during the first three postnatal months (Gerding et al., 2011). In the WT mouse retina, CCDC66 protein expression is present directly after birth and during early postnatal development. In conjunction with the early signs of degeneration in the photoreceptors, these studies demonstrate the crucial role of CCDC66 protein in retinal development and function.

Recent research suggests that CCDC66 plays a role in microtubule-mediated functions in terms of spindle pole and centriolar satellite organization as well as in cilium formation and trafficking, which hints to multiple functions of CCDC66 protein also outside of the retina (Sharp et al., 2011; Conkar et al., 2017). An initial screen of *Ccdc66* RNA expression by quantitative real-time polymerase chain reaction (PCR) confirmed extra-retinal *Ccdc66* RNA expression also in the WT mouse brain (Dekomien et al., 2010). The relevance of *Ccdc66* gene expression and its products outside of the retina, more specifically in the brain, and the consequences if CCDC66 protein is absent, are still unclear; the *Ccdc66* -/- mouse does not show an obvious phenotype such as seizures, freezing or overall impaired locomotion that might be related to major brain damage. In turn, if there are effects due to a lack of proper *Ccdc66* gene expression, these are rather expected to be mild, subtle and/or to manifest later in life.

The present study therefore aimed at characterizing CCDC66 protein-expressing structures in the WT mouse brain and to uncover whether the lack of *Ccdc66* gene expression in the *Ccdc66* -/- brain might result in morphological and behavioral alterations. Thereby, this study heralds further insights into the function of CCDC66 protein.

Experimental procedures

Animals

Ccdc66 -/- mice were generated and genotyped as described before (Gerding et al., 2011). In short, the transgenic *Ccdc66* -/- mouse, is a knock-in model, where a trap has been introduced in the 5′ end of mouse exon 4 (accession no. NM_177111). The gene trap consists of a splice acceptor site, a β-galactosidase/neomycin phosphotransferase fusion gene (ßgeo) and a bovine polyadenylation site, resulting in a fusion protein of CCDC66, encoded by the first three exons of the gene, and β-galactosidase. Mice homozygous for the mutant *Ccdc66* lack two functional copies of the full-length *Ccdc66* gene (*Ccdc66*-deficient or *Ccdc66* -/-). Mice of the C57BL/6 J strain were obtained from the Jackson Laboratory (Bar Harbor, ME, USA), bred at the Ruhr-University Bochum, Germany, and kept in a light/dark cycle of 12/12 h. *Ccdc66* -/- mice were backcrossed to a C57BL/6 J background to at least generation 7. The animals had unlimited access to commercial food and water. All experimental procedures complied with the German guidelines for animal care and were approved by the regional authority (LANUV, North-Rhine Westphalia, Germany; reference number 84-02.04.2015.A250).

Tissue preparation

Mice were deeply anesthetized with CO_2 and decapitated. Brain and retina tissue was dissected and immediately frozen on dry ice (for protein isolation) or in isopentane on dry ice (for X-gal staining/reporter gene visualisation). Tissues were stored at −80 °C until further use. The day of birth was defined as P0. For protein isolation, tissues from WT mice (*Ccdc66* +/+; n = 3/age) were pooled at each investigated age. Retinas were collected at 3 months, and brain hemispheres at 3 months and postnatal days P4, P8, P10, P12, P15, P19, and P24. For X-gal staining, olfactory bulbs from P4, P10, P17, 1 month, 1.5 months- and over 10-month-old *Ccdc66* -/- mice and WT controls (n = 3/age and genotype) were embedded in freezing medium and snap frozen for cryosectioning. In addition, whole mount preparations of the olfactory bulb and epithelium of an adult *Ccdc66* -/- and an age-matched WT mouse were investigated by the removal of nasal, frontal and parietal bones, immediately followed by X-gal staining (see below). For electron microscopy, *Ccdc66* -/- and age-matched WT mice (n = 3/genotype and age; 1, 3, 9, 12 and 18 months) were anesthetized by pentobarbital-potassium (500 mg/kg Narcoren®, Merial GmbH, Germany) and perfusion-fixed with 2.5% glutaraldehyde in 0.1 M phosphate buffer (pH 7.4) for 20 min and transferred into 0,5% PFA until used.

Western blot analysis

Western blot analysis was conducted as described previously. Briefly, homogenates from mouse tissue were extracted in ice-cold radioimmunoprecipitation assay (RIPA) buffer (50 mM Tris - HCl (pH 8.0), 150 mM NaCl, 1% (v/v) NP-40, 1 g/l SDS, 1 g/l Na-Desoxycholate) with a protease inhibitor cocktail (Sigma-Aldrich, USA) on ice for 20 min, centrifuged at 600 *g* for 20 min, and supernatants were harvested and stored at −80 °C. Protein quantification was performed according to a standard method (Pierce™ BCA Protein Assay Kit, #23225, Thermo Scientific™, USA), following the manufacturer´s protocol. Samples were adjusted to equal volumes with RIPA buffer and denatured in Laemmli-buffer (31% (v/v) 5.5 M Tris (pH 6.8), 10% (w/v) SDS, 50% (v/v) glycerol) at 95 °C including a final concentration of 100 mM DL-Dithiothreitol (DTT). Protein (40 µg) was loaded on 10% SDS-PAGE and transferred onto a nitrocellulose membrane (Hybond C, GE Healthcare, Germany). Unspecific binding sites on the membrane were saturated by incubation with a blocking reagent (Western Blocking Reagent, Solution, Sigma-Aldrich) followed by incubation with the primary antibody diluted in phosphate-buffered saline (PBS) and blocking reagent (1:1; polyclonal rabbit anti-CCDC66 antibody, T-20, Santa Cruz Biotechnology Inc. (1:200)). Using horseradish peroxidise- (HRP-) conjugated goat anti-rabbit antibody (1:5000; Jackson ImmunoResearch, USA), detection was carried out using ECL plus (GE Healthcare, UK) and documented by using the FUSION-SL documentation system and FUSION-CAPT software (VWR, Germany). Antibodies were removed with stripping buffer (Restore™ Western Blot Stripping Buffer, Thermo Scientific™, USA) and re-probed with antibodies for loading control (anti-glyceraldehyde-3-phosphate dehydrogenase (GAPDH; rabbit, polyclonal IgG, #ab9485, 1:500, Abcam, UK)). The relative protein expression was quantified using the ImageJ 1.35i analysis tool (Wayne Rasband, National Institutes of Health, USA) (Schindelin et al., 2015) by measuring the integrated optical density of bands and subsequent normalization to GAPDH expression.

X-gal staining

Ccdc66 reporter gene-positive cells were labelled by the blue precipitate released during the hydrolysis reaction of X-gal through the

lacZ-encoded β-galactosidase. Frontal cryosections (30 µm; CM1850 Cryostat, Leica, Germany) were dried at room temperature (RT), briefly fixed in EtOH (7 min, −20 °C), transferred into PBS (5 min, RT), covered with 500 µl of 20 mg/ml X-gal staining solution (in 9.1 ml PBS, 100 µl 500 mM $K_3Fe(CN)6$, 100 µl 500 mM K4 Fe(CN)6, 200 µl 100 mM $MgCl_2$) and incubated overnight at 37 °C in a humidity chamber. Sections were slightly counter-stained with neutral red solution (0.3% (w/v) neutral red, 0.1 M acetic acid in H_2O) for 3 min, rinsed with H_2O and washed in PBS for 5 min. Finally, tissue dehydration was conducted in ascending EtOH concentrations (70%, 80%, 90%, 96%, 2 × 100%) and sections were cover-slipped in embedding medium (Eindeckmittel DT500, DiaTec, Germany). Images were taken with the Metafer/Vslide system (Metasystems, Germany). Whole mount preparations were immediately incubated in X-gal staining solution (for 1–4 h) and photo-documented with the Olympus Microscope BH-2.

Light and electron microscopy analysis

Light- and electron microscopy analyses were performed as described before (Petrasch-Parwez et al., 2007). Briefly, removed brains were adjusted in a plexiglass frame, embedded in 2% agarose in PBS and cut into 1 mm coronal slices with a vibratome cutter. Slices with the two main olfactory bulbs were photo-documented in PBS (Fig. 4A and C), then postfixed with 4% osmium tetroxide in PBS for 3 h and embedded in araldite. One side was taken for series of semithin sections to investigate morphological alterations light microscopically (Fig. 4B, D, E–H), the other side was taken for alternate semi- and ultrathin sections for electron microscopic analyses (Fig. 5). Semithin sections (0.75 µm) were stained with 1% toluidine blue. Ultrathin sections (100 nm) were contrasted with uranyl acetate and lead citrate. Photo-documentation of semithin sections was performed by an Olympus Microscope BH-2 equipped with an Olympus camera DP-71 (Olympus, Japan) and the computer-assisted software analysis Cell A (Soft imaging system GmbH, Germany). Ultrathin sections were viewed in a Philips EM 420 electron microscope. All data were exported as TIFF files into Adobe Photoshop CS5 Extended (*vs*.12.04 × 64; Adobe Imaging Systems Inc., USA) for documentation. Images used in the same figure were adjusted for brightness and contrast in Adobe Photoshop.

Olfaction habituation/dishabituation test

The olfaction habituation/dishabituation test was performed as described previously (Yang and Crawley, 2009). Shortly, the test consisted of a familiarization phase and a test phase. In the familiarization phase, mice were placed in the testing cage (Scanbur, Denmark) for 30 min while a clean cotton swab (Hain Lifescience GmbH, Germany) was presented. In the test phase in total 5 odors including water, two unknown neutral odors (almond, lemon) and two social scents (social a and social b) were presented 3 times each for 2 min (order: 3× water, 3× almond, 3× lemon, 3× social a, 3× social b). After each 2 min presentation, of both, the same or a new odor, a 1-min pause followed. For each test session 50 µl H_2O or 50 µl of a 1:100 dilution of the odor solutions in H_2O (almond and citrus baking flavors, RUF, Germany; freshly prepared for each test session) were pipetted onto a new cotton applicator directly before the test phase and sealed in a closed tube until the presentation. We focused on the analysis of a single sex (females). Animals of both genotypes, WT and *Ccdc66* -/- were around 1.5 years old (19–21 months of age, which corresponds to the equivalent of the menopausal age in humans (Brinton, 2012). Unfamiliar social scents were prepared on the test day by swapping the bottom of a cage with a mouse from the opposite sex (here male) on a cotton applicator and kept sealed until the presentation. The designations "social a" and "social b" refer to odor samples from the opposite sex (here males) from two different cages (cage 1 = social a, cage 2 = social b). The sniffing duration of each individual at the cotton swab, indicated by the close proximity of the nose to the swab, was recorded in each session with a silenced stopwatch. To ensure accuracy in the recording of the sniffing time, some animals were evaluated simultaneously by two experimenters, which yielded comparable results.

Statistical analysis

One-way ANOVA followed by Tukey post-hoc test was performed to compare protein expression levels across different developmental stages and between different brain regions in the *Ccdc66* +/+ statistically. Statistical evaluation was performed by the Mann-Whitney Rank Sum Test to compare *Ccdc66* +/+ and *Ccdc66* -/- at first odor presentation. The Wilcoxon signed-rank test was used to assess odor habituation in WT and *Ccdc66* -/- by comparing first and third presentations of the same odor and to evaluate dishabituation/discrimination by the comparison of first and third presentations of two different odors. P-values < 0.05 were considered as statistically significant.

Results

CCDC66 protein is present throughout early postnatal development and at high levels in the adult WT olfactory bulb

In order to confirm CCDC66 protein expression in the WT mouse brain, whole-brain and retinal homogenates of 3-month-old mice were assessed by Western blot using a previously validated antibody against protein CCDC66 (Gerding et al., 2011). Besides the strong CCDC66-specific signal detected in the WT mouse retina, protein CCDC66 was also confirmed in the WT mouse brain, while it was not present in the *Ccdc66*-deficient mouse brain (Fig. 1A).

In a former study, it was shown that CCDC66 protein plays a crucial role in the early postnatal development of the mouse retina (Gerding et al., 2011). In order to evaluate a possible role of CCDC66 also in the maturing brain, the developmental time course of CCDC66 protein expression during early postnatal development of the WT mouse brain was assessed by quantitative Western blot analysis (postnatal days P4, P8, P10, P12, P15, P19, P24; Fig. 1B). CCDC66 protein was present at significantly lower levels at all investigated stages with the exception of P4, compared to its expression in the adult retina (Fig. 1B). To define CCDC66 protein-rich brain regions, homogenates from different brain regions of adult WT mice were analyzed by Western blot (Fig. 1C). Remarkably, the amount of CCDC66 protein detected in the olfactory bulb was comparable to the CCDC66 protein level in the retina. Compared to the adult retina and the olfactory bulb, less CCDC66 protein was present in other brain regions analyzed (brain stem, cerebellum, cortex, striatum and hippocampus; Fig. 1C).

Since background staining complicated the immunohistochemical detection of specific signals in mouse brain sections using the previously validated anti-CCDC66 antibody (Dekomien et al., 2010; Gerding et al., 2011) the detection of *Ccdc66* gene products in the brain was performed indirectly by X-gal staining. As CCDC66 protein is prominently expressed in the WT mouse olfactory bulb, the focus of assessing reporter gene expression in the *Ccdc66* -/- mouse brain was on the olfactory bulb and selected olfaction-associated structures.

Ccdc66 reporter gene expression in the adult Ccdc66 -/- olfactory system

Ccdc66 -/- adult mice showed intense *Ccdc66* reporter gene expression in the olfactory bulb and the olfactory epithelium, as shown by X-gal staining in whole mount preparations (Fig. 2A), whereas the WT control lacked X-gal staining (Fig. 2B). The *Ccdc66* -/- olfactory epithelium revealed *Ccdc66* gene expression predominantly in the layer of the olfactory receptor neuron cell bodies and most likely along their apical dendrites appearing as intensely labeled processes between the supporting cells (Fig. 2C). Expression might be either in the somata and/or in the passing processes of the olfactory receptor neurons. In coronal sections of the main olfactory bulb of adult *Ccdc66* -/- mice, X-

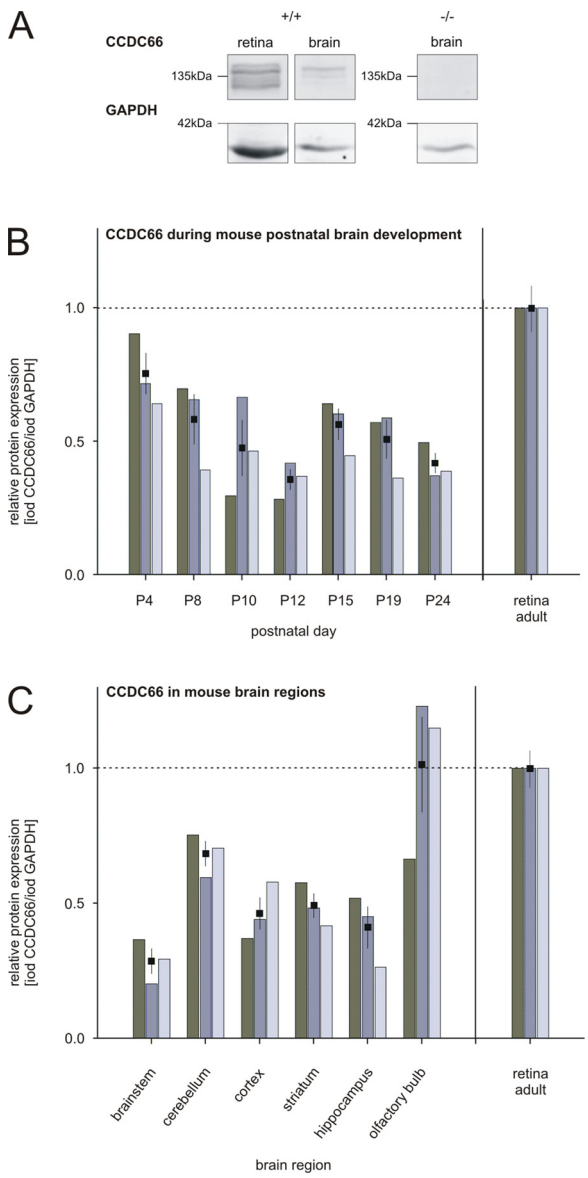

Fig. 1. Quantitative CCDC66 protein expression in the developing and adult wild-type mouse brain.
A) Western blot analyses of brain and retinal homogenates from 3-month-old wild-type (WT; +/+) mice revealed the high molecular weight signal of CCDC66 protein at ~100-140 kDa, while no signal was detectable in the *Ccdc66*-deficient (-/-) mouse brain. GAPDH was probed as loading control. B) CCDC66 signals in early postnatal WT mouse brain homogenates were normalized to GAPDH, and the CCDC66 expression level in the adult retina was set to 1. Compared to the adult mouse retina, significantly lower amount of protein CCDC66 was measured in brain homogenates at all ages analyzed, except for P4 (P8, P10, P12, P15, P19, P24; $p < 0.05$). C) Quantitative CCDC66 protein expression in different brain regions of adult WT mice (normalized and compared as in B) showed highest CCDC66 expression levels in the olfactory bulb and the cerebellum, compared to the adult mouse retina. In the cortex, striatum, brainstem and hippocampus significantly less CCDC66 protein was detected ($p < 0.05$). N = 3 were analyzed in three independent experiments per developmental stage, each experiment depicted in a different color. iod = integrated optic density. Each bar represents one experiment, squares represent mean values. Error bars = standard error of the mean.

gal staining showed intense *Ccdc66* reporter gene expression in the olfactory nerve layer, the olfactory glomeruli (Fig. 2D, enlarged in 2E) and in the subependymal zone (Fig. 2D, magnified in 2F). In a sagittal section of the *Ccdc66* -/- forebrain, *Ccdc66* reporter gene was visualized along the region of the rostral migratory stream including the area of the subventricular zone (Fig. 2G, magnified in 2H).

Spatiotemporal Ccdc66 reporter gene expression during postnatal development of the Ccdc66 -/- main olfactory bulb

Western blot analyses of whole brain homogenates at different postnatal ages suggest a developmental change in CCDC66 protein expression in the WT mouse brain. Of note, in the adult WT mouse, CCDC66 protein in the olfactory bulb was expressed at similar levels as in the retina. In addition, *Ccdc66* reporter was highly expressed in the adult *Ccdc66* -/- mouse primary olfactory system. In order to capture developmental dynamics of *Ccdc66* reporter gene expression in the olfactory bulb, X-gal staining was performed throughout the early postnatal development of the *Ccdc66* -/- mouse olfactory bulb. Interestingly, *Ccdc66* reporter gene expression was present at all investigated stages, predominantly in the olfactory nerve layer, as early as P4 and continuing at P10, P17, 1 month, 1.5 months and after 10 months (Fig. 3). Staining is thereby predominantly visible on the medial and ventral surface of the olfactory bulbs, where the olfactory nerve layer is more prominent compared to the dorsal (and lateral) surface. In addition, reporter gene seemed to successively increase in the olfactory glomeruli from about 1 month of age (Fig. 3D, enlarged in 3J) to over 10 months of age (Fig. 3F, enlarged in 3L), in the latter also with intense labeling of the dorsal olfactory bulb glomeruli. Reporter gene expression in the olfactory glomeruli was not observed in P4 to P17 (Fig. 3A–F). Hence the first occurrence of reporter gene expression in the glomeruli became obvious after their initial formation during embryonic development with numerous glomeruli already formed at P4 (Blanchart et al., 2008; Treloar et al., 2010), but *Ccdc66* expression increased with progressing maturation of the glomeruli with their dense innervation and synapses formation (Pomeroy et al., 1990). At P4 and P17, the subependymal zone also showed *Ccdc66* reporter gene expression (Fig. 3A and C).

Ccdc66-deficient mice showed degeneration of olfactory nerve fibers in the olfactory bulb

To investigate whether impaired expression of functional *Ccdc66* gene products leads to degeneration in the main olfactory bulb, 1-, 3-, 9-, 12- and 18-month-old *Ccdc66* -/- and +/+ brains were investigated by semi- and ultrathin section series. In semithin sections, neither at the young nor at the old ages, morphological differences were observed between the *Ccdc66* -/- and +/+ olfactory bulbs (Fig. 4). In both genotypes, the olfactory bulbs displayed regular external and internal plexiform layers (Fig. 4E and F). The large mitral cells in between showed light neuronal somata and thick dendrites emerging towards the external plexiform layer. Dark cell degeneration, a characteristic phenomenon of dying cells in neurodegeneration (Turmaine et al., 2000; Nuber et al., 2008), which can easily be detected in Toluidine blue-stained semithin sections, was not observed. The glomerular cell layer (Fig. 4G and H), which was closer inspected according to its strong X-Gal staining at advanced ages, showed the characteristic darkly appearing unmyelinated nerve fibers entering the glomerula from the olfactory nerve layer. They terminate at the dendrites, which are localized in the lighter patchy parts of the glomerular neuropil. To note, semithin section series revealed no signs of degeneration in the main olfactory bulbs in *Ccdc66* -/- mice.

Electron microscopic analyses revealed that *Ccdc66* -/- mice exhibited normal olfactory bulb morphology at 1 month, when compared with *Ccdc66* +/+ mice (data not shown). At 3 months of age (Fig. 5A), solitary accumulations of single or double membrane vesicular formations (autophagic-like structures) occurred in the *Ccdc66* -/- glomerular layer, some of which filled with dense material. Because these accumulations were so rare it was not possible to determine where they are subcellulary localized. At advanced age (9, 12 and 18 months), it became obvious, that the accumulations of autophagic-like vesicles were abundantly localized in the glomerular

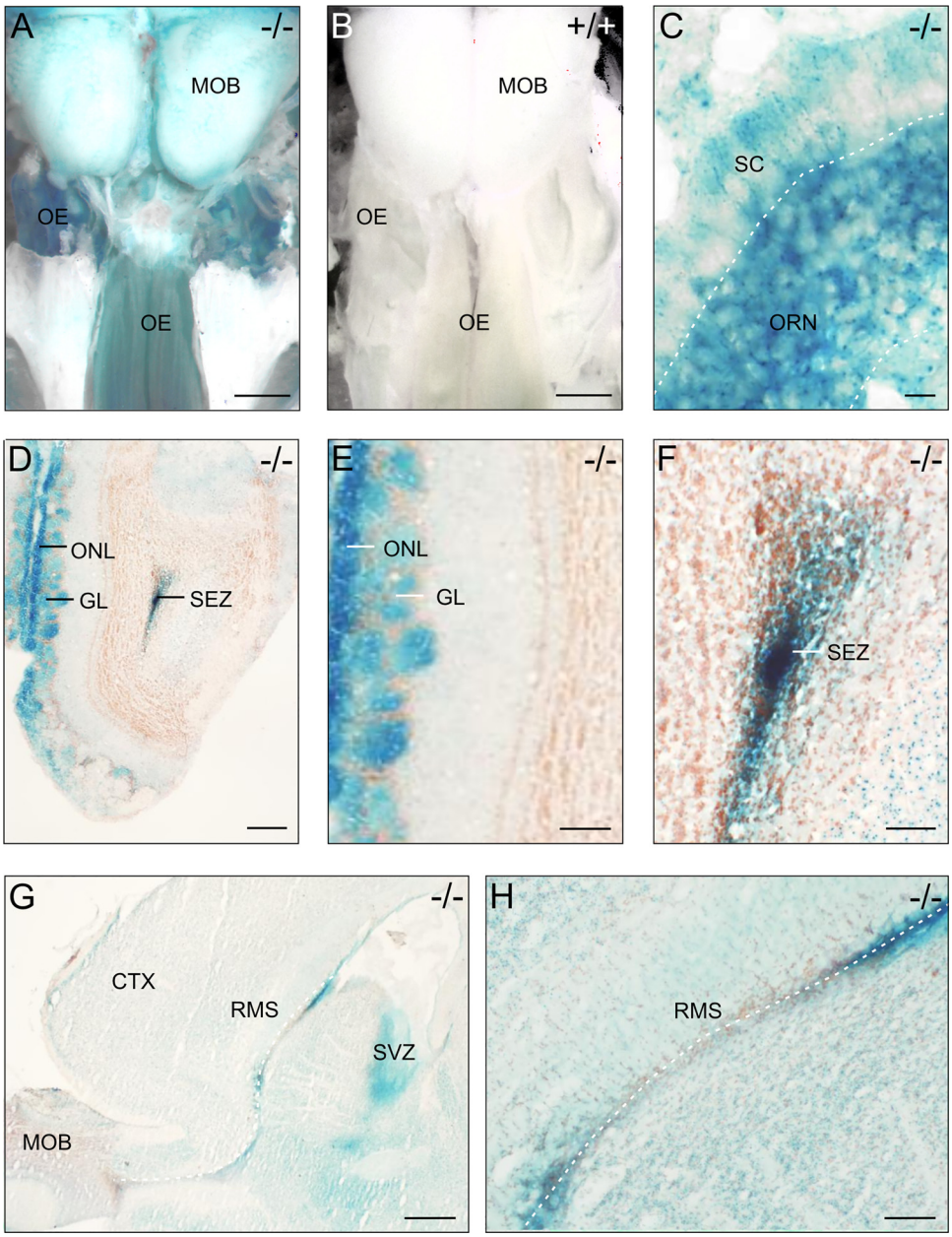

Fig. 2. *Ccdc66* reporter gene expression in parts of the *Ccdc66* -/- olfactory system. **A**) The 10-month-old *Ccdc66* -/- mouse olfactory epithelium (OE) and main olfactory bulb (MOB) revealed strong, distinct labeling in contrast to the WT (+/+) littermate control **(B)** shown by X-gal staining of whole mount MOB/OE-preparations. **C)** *Ccdc66* reporter gene expression was localized in the cell body layer of the olfactory receptor neurons (ORN) in the *Ccdc66* -/- epithelium as well as along the thin dendrites running between the weakly stained supporting cells (SC) towards the epithelial surface. **D)** Frontal cryosections of the MOB revealed prominent X-gal staining in the olfactory nerve layer (ONL) and the glomerular layer (GL; enlarged in **E)** as well as in the subependymal zone (SEZ; enlarged in **F**). **G)** Sagittal cryosections of a 1.5 month-old *Ccdc66* -/- brain showed X-gal staining in the subventricular zone (SVZ) and partially in the region along the rostral migratory stream (RMS; enlarged in **H**). CTX – cortex. Cryosections are slightly counterstained with neutral red. Scale bar in A, B, G: 1 mm, in C: 10 µm, in D: 200 µm, in E: 100 µm, in H, F: 50 µm.

layer (Fig. 5C, 12 months). They were mainly embedded in the dark axoplasm of the unmyelinated olfactory nerve fibers within the glomeruli (Fig. 5C and E). The accumulations may lead to expansions in these otherwise thin axons. Most vesicles presented with double membranes confirming the character of autophagosomes (Fig. 5E). Some terminals filled with autophagosomes formed synaptic contacts with dendritic processes (Fig. 5F). *Ccdc66* +/+ controls lacked degenerations at any stage analyzed (Fig. 5B and D). The electron microscopic findings indicate, that autophagy contributes to axonal degeneration in Ccdc66 -/- mice at advanced age focused on the glomerular olfactory nerve fibers and their terminals, suggesting an impairment of olfactory transmission in *Ccdc66* -/- mice at advanced age.

Degeneration of the olfactory bulb glomeruli in Ccdc66 -/- mice results in impaired olfactory performance

Based on the degeneration in the olfactory bulb of adult *Ccdc66* -/- mice at advanced age (Fig. 5), olfaction habituation and dishabituation (discrimination) was analyzed to determine whether functional changes in the olfactory performance of *Ccdc66* -/- mice might be caused by neurodegeneration in the olfactory bulb. The test measures behavioral responses to the presentation of neutral non-social as well as social scents from the opposite sex (here males). *Ccdc66* -/- mice spent significantly less time sniffing a new scent than did WT controls, except for the presentation of the non-social almond odor (Fig. 6A, p-values in 6C). WT and *Ccdc66* -/- showed (at least a tendency towards) habituation to neutral, non-social odors observed by a gradually reduced response with increasing repetition of odor presentation (Fig. 6B, p-values in 6C). WT mice also tended to habituate to social odors, while *Ccdc66* -/- mice barely showed any reaction and therefore no habituation (Fig. 6B, p-values in 6C). In addition, compared to the WT, the *Ccdc66* -/- mouse showed reduced discrimination performance of the presented odors as revealed by, in most cases, non-significant changes in sniffing time between third and subsequent first presentation of the next odor (Fig. 6B, p-values in 6C).

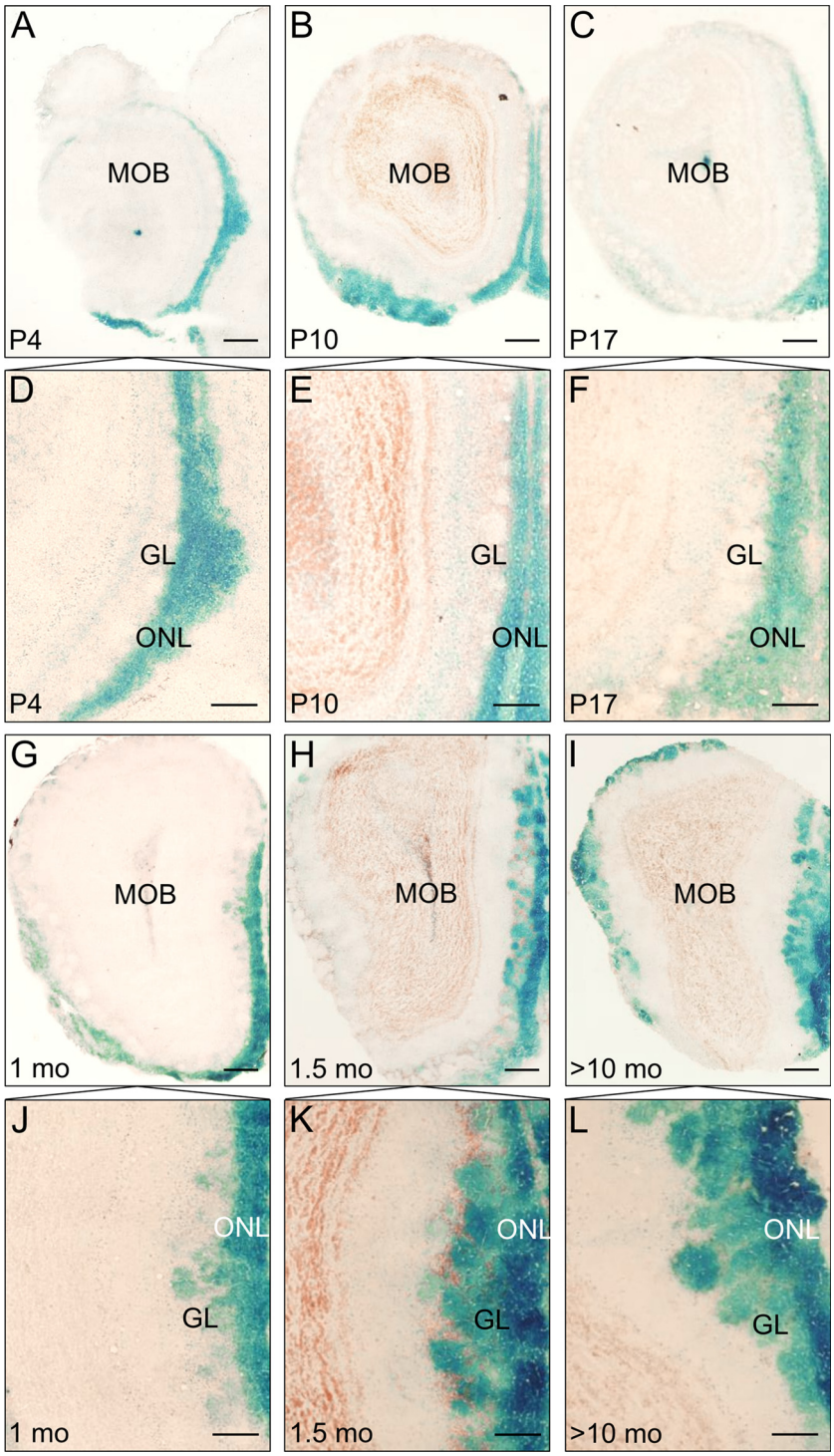

Fig. 3. *Ccdc66* reporter gene expression during postnatal development of the *Ccdc66* -/- mouse olfactory bulb.
Frontal cryosections of the main olfactory bulb (MOB) slightly counterstained with neutral red showed blue X-gal staining precipitates at all investigated postnatal stages: P4 (**A, D**), P10 (**B, E**), P17 (**C, F**), 1 month (**G, J**), 1.5 months (**H, K**) and > 10 months (**I, L**). During the first month, staining was restricted to the olfactory nerve layer (ONL). Labeling of the glomerular layer (GL) started around 1 month of age (**G, J**) increasing with age (**H, K** and **I, L**). Remaining layers of the olfactory bulb lacked gene expression. Scale bar in A–C, G-I: 200 µm, in D–F, JL:100 µm.

Discussion

The genetically modified *Ccdc66* -/- mouse exhibits early photoreceptor loss with slow progressive retinal degeneration and functional impairment of the retina (Gerding et al., 2011). Here we report that the lack of functional *Ccdc66* gene expression results in degeneration of the olfactory nerve fibers in the olfactory bulb glomeruli as well as in altered olfactory performance in *Ccdc66* -/- mice. The present findings categorize the *Ccdc66* -/- mouse as a model for cerebral neurodegeneration, in addition to the previously reported retinal degeneration.

CCDC66 protein/Ccdc66 reporter gene expression in the olfactory bulb

The results show that CCDC66 is not only expressed in the retina, but also in the WT mouse brain during postnatal development, primarily in the olfactory system. Of note, among different brain regions of the adult WT mouse brain, the olfactory bulb exhibited levels of CCDC66 protein expression comparable to those in the retina. Likewise, the *Ccdc66* -/- mouse displayed strong and distinct *Ccdc66* reporter gene expression in the olfactory bulb glomeruli and the nerve fibers as well as in the olfactory epithelium. Moreover, *Ccdc66* reporter gene expression could be visualized along the pathway of the rostral migratory stream, *i.e.* the path of constant supplement of migrating

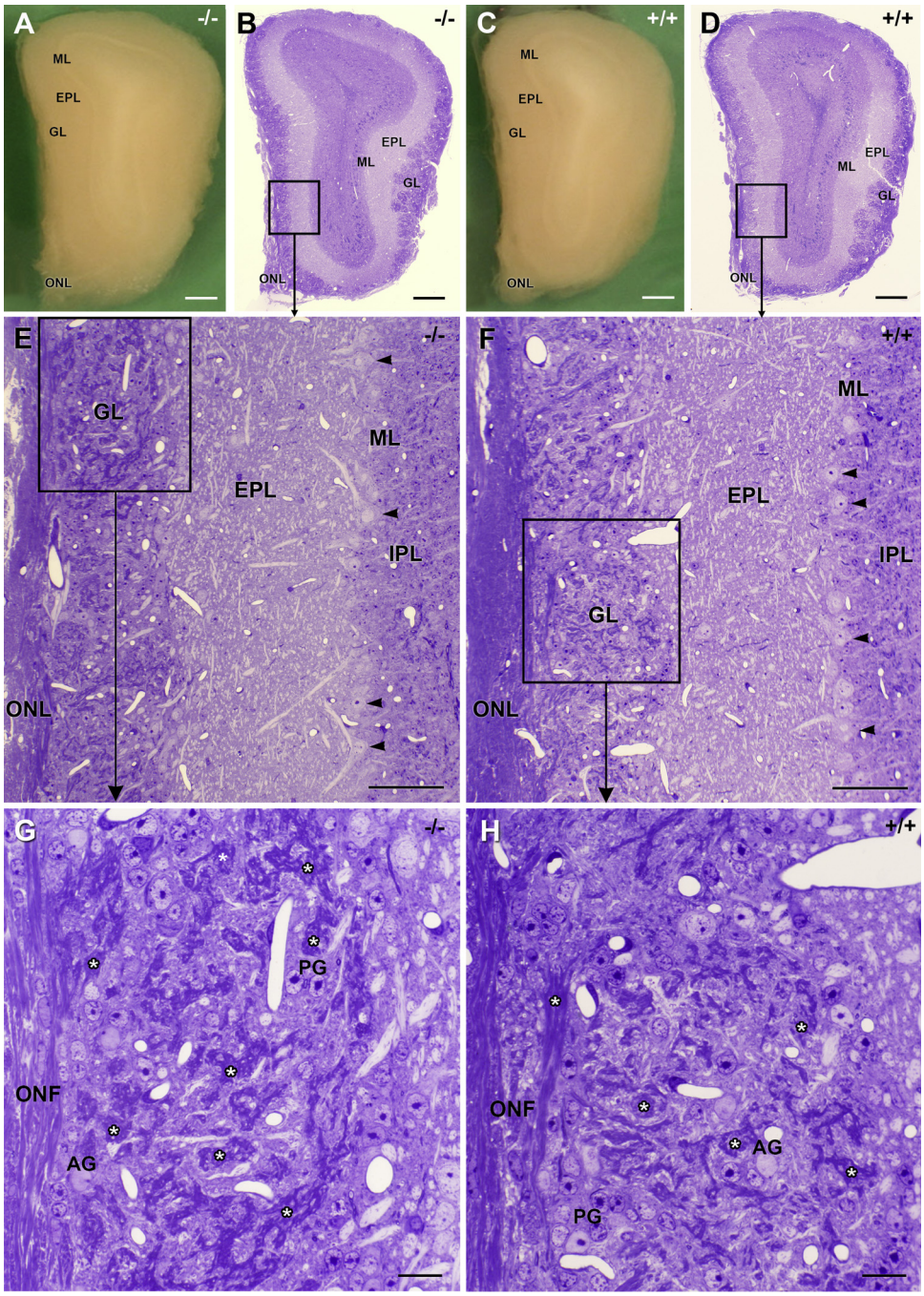

Fig. 4. Light microscopy of the olfactory bulb of *Ccdc66* -/- and *Ccdc66* +/+ mice.
Main olfactory bulb slices (1 mm) of 12 month-old *Ccdc66* -/- **(A)** and *Ccdc66* +/+ mice **(C)** were photo-documented in PBS for later orientation. The mitral cell layer (ML) is indicated as a light stripe bordered laterally of the external plexiform (EPL) and glomerular layer (GL). Semithin section series from these embedded slices showed normal olfactory bulb morphology in both genotypes as documented in overview pictures **(B, D)** and enlargements **(E, F, G, H).** The olfactory bulb displayed regular internal plexiform layer (IPL) and EPL in the *Ccdc66* -/- **(E)** and +/+ **(F)** - olfactory bulbs with large light mitral cell somata (black arrowheads) in between with no differences in morphological appearance between the genotypes. **G/H**) Dark appearing unmyelinated nerve fiber bundles (asterisks) emerging from the olfactory nerve layer (ONL) are distributed in the GL between the light neuropil patches comprising dendrites, astrocytes (AG) and associated periglomerular cells (PG). Differences between *Ccdc66* -/- and +/+ with evidences of pathologies in the -/- glomeruli were not observed in semithin sections. Scale bar in **A, B, C, D**: 200 µm, in **E, F**: 50 µm, in **G, H**: 10 µm.

neuronal precursors that differentiate in granule and periglomerular cells in the respective layers of the olfactory bulb (Lois and Alvarez-BuyIIa, 1994; Kornack and Rakic, 2001; Curtis et al., 2007). Interestingly, in the olfactory nerve layer and olfactory bulb glomeruli, *Ccdc66* reporter gene expression qualitatively increased during postnatal development. This is in contrast to the decreasing expression of CCDC66 protein in the WT mouse brain; however, CCDC66 protein expression levels were not analyzed in the different brain regions separately so that an increase of the CCDC66 protein level in the olfactory bulb might be obscured by a decrease of CCDC66 expression in other brain regions.

Despite the limited spatial resolution of enzymatic X-gal staining, distinct *Ccdc66*-reporter gene expression was observed in the olfactory nerve layer and olfactory bulb glomeruli where the olfactory nerve fibers terminate. More specifically, *Ccdc66* gene expression in the nerve fiber layer of the olfactory bulb is present soon after birth, while labeling of the glomeruli does not start with the presence of the first mature glomeruli that are present prior to birth (Blanchart et al., 2008), but coincides or increases along with maturation of the glomeruli, reflected *e.g.* by increased glomeruli innervation and respective synapse formation (Pomeroy et al., 1990). *Ccdc66* expression in the olfactory bulb glomeruli starts appearing at the age of 1 month. Besides increased innervation, a developmental event that might parallel the developmental time course of *Ccdc66* -/- olfactory glomeruli labeling could be the turnover of olfactory receptor neurons. There has been controversy in reports on the lifespan of olfactory sensory neurons in mice, from approximately one month up to 90 days or even longer (Graziadei and Graziadei, 1979; Wilson and Raisman, 1980; Hinds et al., 1984; Mackay-Sim and Kitte, 1991; Kondo et al., 2010). However, the turnover of the olfactory receptor neurons goes along with the process of remodeling, which might be consistent with the proposed function of

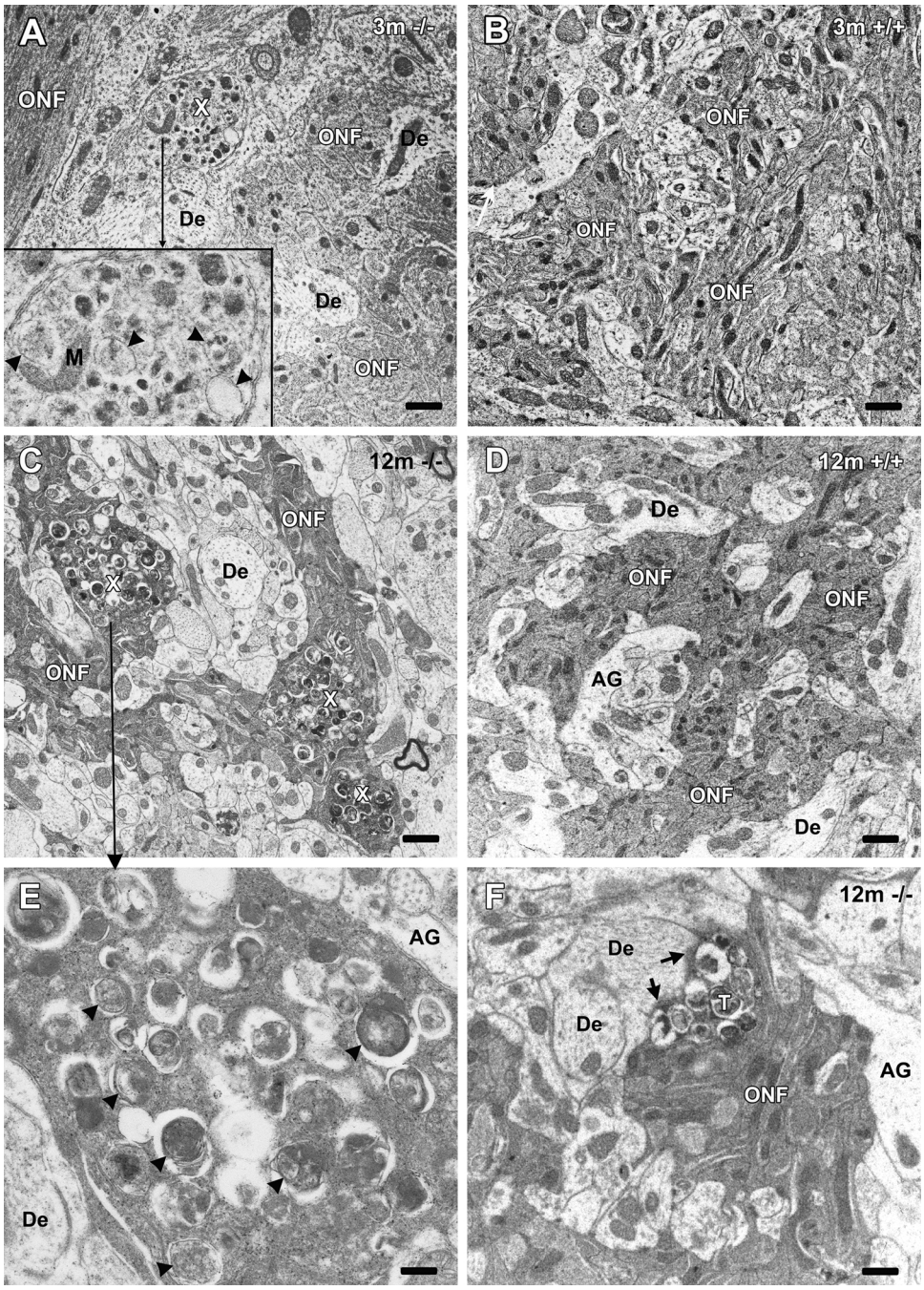

Fig. 5. Electron microscopy of the olfactory bulb glomeruli in *Ccdc66* -/- and *Ccdc66* +/+ mice.
A) Ultrathin section of 3 month-old *Ccdc66* -/- glomeruli revealed single rounded structures (x) with accumulations of membrane-surrounded autophagic-like vesicles (black arrowheads in the enlarged inlay in **A**), some of which filled with electron-dense deposits corresponding to autophagosomes, not observed in age-matched *Ccdc66* +/+ mice **(B)**. **C)** At 12 months of age, multiple structures with these autophagic-like vesicles are mainly localized in the dark appearing unmyelinated glomerular olfactory nerve fibers (ONF), not detected in age-matched *Ccdc66* +/+ (**D**).
E) Enlargement of **C** showed many vesicles surrounded by membranes (arrowheads) within the dark axoplasm of the ONF. **F)** Autophagic-like vesicles were also detected in synaptic terminals (T) contacting a dendrite (De). Two postsynaptic densities are marked by arrows. AG, astroglia. M, mitochrondion. Scale bar in **A, B, C, D**: 1 µm, in **E, F**: 0.2 µm.

CCDC66 being involved in cytoskeleton remodeling (Conkar et al., 2017). Furthermore, *Ccdc66* reporter gene expression in the ciliated olfactory sensory neurons strengthens the recently published finding that CCDC66 is involved in cilium formation and trafficking (Conkar et al., 2017).

Degeneration in the olfactory bulb of the Ccdc66 -/- mouse

Ccdc66 -/- mice exhibit reporter gene expression in the olfactory epithelium, the olfactory nerve fibers and in the adult olfactory glomeruli. Accumulations of autophagic-like structures were observed in the olfactory nerve fibers within the glomeruli at advanced age, suggesting an olfactory impairment in the first relay station of the olfactory pathway. It is not clear whether the olfactory epithelium also degenerates. The primary focus of this study concerns the olfactory bulb showing degenerations at advanced age. Degeneration of the axon terminals of the olfactory sensory neurons due to prior degeneration of the olfactory cilia could represent a possible degeneration mechanism and will be subject of further studies.

Interestingly, the autophagic-like vesicles in the olfactory nerve fibers were not found in 1-month-old *Ccdc66* -/- mice, it starts at the age of three months with single degeneration signs. This is consistent with the *Ccdc66* reporter gene being expressed in the *Ccdc66* -/- olfactory glomeruli just starting in 1-month-old mice and increasing with age. We did not investigate ages between 3 and 9 months old, but it is likely that the crucial development of dystrophic axons happens in that time window. We realize that the statistical evaluation of the degeneration is very important and should be addressed in our future studies with a special focus on the development of the degeneration together with specific immunohistochemical and additional functional studies.

A potential spatiotemporal process coinciding *Ccdc66* expression might be the maturation of the olfactory glomeruli, the turnover of

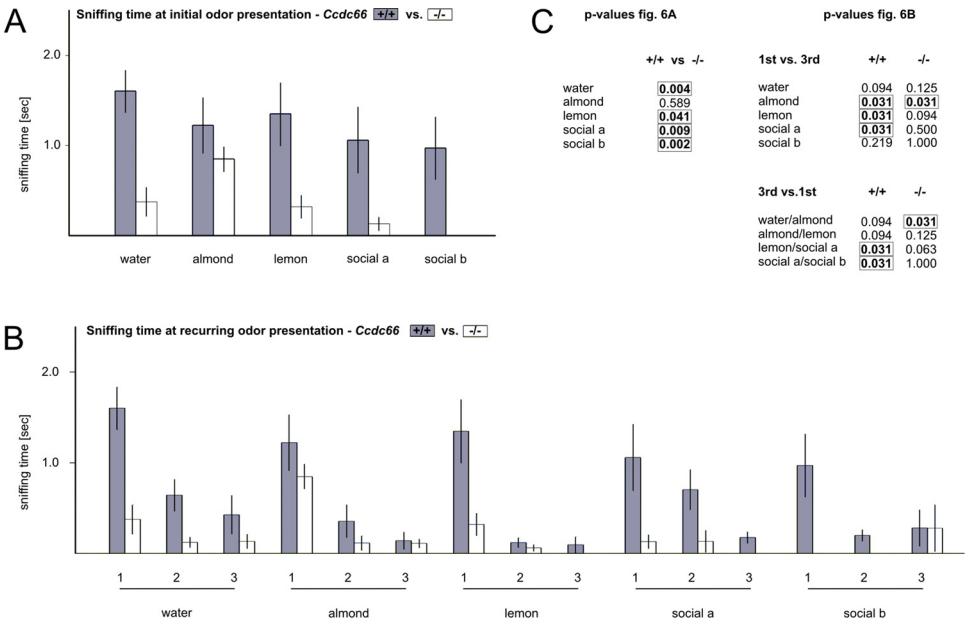

Fig. 6. Olfactory performance of WT and *Ccdc66* -/- mice in a habituation/dishabituation test.
A) In comparison to *Ccdc66* +/+ controls, *Ccdc66* -/- mice spent significantly less time sniffing at initial odor presentation except for the almond odor where they showed only a tendency towards decreased sniffing (for p-values see overview in C; significant changes are in bold and framed). **B)** A tendency to habituate to neutral odors was present in both, *Ccdc66* +/+ and *Ccdc66* -/- mice, as shown by the decreasing sniffing time along with increasing repetition of odor presentation (for p-values see table in **C)**, significant changes are in bold type and framed). Dishabituation/discrimination was assessed by significant changes between third presentation of an odor and first presentation of the next odor. *Ccdc66* +/+ mice tend to discriminate neutral, non-social and social odors from the opposite sex (two different males (social a; social b)) and to habituate to social odors while *Ccdc66* -/- mice barely even responded to the social odors. Each bar represents mean values from n = 6 animals. Error bars = standard error of the mean.

olfactory sensory neurons (see previous section), or more generally the process of renewal, that initiates degeneration in some *Ccdc66*-deficient structures. In the retina, for example, CCDC66 protein is present in the outer segments of retinal photoreceptors prior to the formation of outer segments that are also permanently renewed (Young, 1967). Initial signs of degeneration in the retina are present from as early as P13, so that proper outer segments do not form at all (Gerding et al., 2011). CCDC66 might be associated with processes involved in cytoskeletal-dynamics, more specifically the process of the renewal or reconstruction of ciliated cells. The fact that retinal photoreceptor cells as well as olfactory sensory neurons, both ciliated cells, undergo degeneration in the *Ccdc66* -/- mouse suggests that a ciliopathy-like disease phenotype might be represented by the *Ccdc66* -/- mouse. The investigation of additional ciliated systems in the *Ccdc66* -/- mouse will be of further interest in following studies.

Olfactory deficits in the Ccdc66 -/- mouse

The impairment of olfactory capacity is often an early sign of neurodegeneration, as it happens to be the case in Parkinson´s or Alzheimer´s disease, and can precede the onset of for example motor symptoms in Parkinson´s disease (Doty, 2012). The early recognition of neurodegeneration, for instance by loss of olfactory sense, is essential for the initiation of neuroprotective therapies (Sarkar et al., 2016). Olfaction is a key sensory modality in mice. The main olfactory bulb that showed degeneration in the *Ccdc66* -/- mice is primarily responsible for the perception of neutral odors, but it also plays a role in the perception of volatile urine odors (Kang et al., 2009). When studying neurodegeneration in the olfactory system, it is generally recommended to test males and females separately in order to identify sex-dependent alterations (Lehmkuhl et al., 2014). In some studies, neurodegeneration due to neurotoxic substance exposure or olfactory changes were more pronounced in females than in males (Roddick et al., 2016). Therefore, we focused on the analysis of a single sex (females) for the habituation/dishabituation test. To detect potential effects, the investigated animals were older than the age at which we confirmed degeneration in the olfactory bulb (*i.e.* > 1.5 years).

The results here showed that the *Ccdc66* -/- mouse, compared to the *Ccdc66* +/+ control, exhibited a decreased ability to detect odors, especially social odors. Besides the degeneration of the olfactory bulb, these effects might also be an effect of the vomeronasal organ/accessory bulb degeneration, which will be of interest in further studies. In general, the olfactory capacity does not seem to be entirely exhausted in the *Ccdc66* -/- mouse, since there is a certain ability to discriminate and habituate also in the *Ccdc66* -/- mouse, and there are some differences regarding the type of presented odor. The presentation of almond did not reach significant differences between first odor presentation in *Ccdc66* +/+ and *Ccdc66* -/- mice. This might be either the result of the technical aspect, respectively the small sample size tested, or, generally different odor qualities or of degeneration in certain areas in the *Ccdc66* -/- mouse. In case that degenerations in the region of the *Ccdc66* -/- olfactory bulb where lemon rather than almond odor patterns are represented, with each odor having a specific pattern in the olfactory bulb odor map, the detection of some odors might be impaired more than others (Sakano, 2010; Mori et al., 2006).

The Ccdc66 mouse as a model for retinal disease, neurodegeneration and beyond?

The *Ccdc66* mouse model, initially presented as a model for RP-like retinal degeneration, could also be useful to study neurodegeneration, which we observed in the olfactory system and which will be investigated in additional brain/organ systems in the future taking into consideration the potential role of CCDC66 in cilia formation and maintenance.

Overall, one of the benefits of the *Ccdc66* -/- mouse model regarding the neurodegeneration in the olfactory bulb and the retina is the slow progression of neurodegeneration that enables a long monitoring period. Furthermore, the homozygous *Ccdc66* mutation is, despite its effects on the visual, olfactory and probably on other systems, not lethal. This implies, in case of additional, yet undiscovered effects in the *Ccdc66* -/- mouse brain, that these effects can be expected to be mild and/or late manifesting and they can be analyzed during a long time span.

In general, the phenotype of animal models might be moderate in comparison to the phenotype of its respective human disease, yet the *Ccdc66* gene is highly conserved in vertebrate species and also expressed in the human retina (Dekomien et al., 2010).

CCDC66 mutation in other species and human disease research

The identified degeneration of the *Ccdc66* -/- olfactory bulb is

mirrored by impaired olfactory behavior in *Ccdc66* -/- mice. Initially the CCDC66 mutation in the mouse model studied here was identified to be associated with gPRA in Schapendoes dogs (Dekomien et al., 2010). Originally for centuries, the Schapendoes were bred as herders and not as scent dogs, while during the last decades they were converted into accompanying dogs exclusively. The affected dogs exhibited a clear retinal phenotype. Regarding the findings presented here, affected dogs' owners were retrospectively interviewed about the dogs' sniffing behavior. According to the owners reports, the sniffing behavior of the Schapendoes dogs seemed not to be obviously affected. On the one hand, the findings in the mouse model are not necessarily unrestrictedly transferrable to the dog species, primarily because we do not know about degenerations in the olfactory bulb of dogs harboring the gPRA-causing *CCDC66* mutation. On the other hand, a potentially slightly altered sniffing behavior could be difficult to assess, especially in daily life, since dogs might sniff but could have an impaired discrimination ability. Furthermore, neither domesticated dogs nor laboratory *Ccdc66* -/- mice do live in an environment with selective pressure. Therefore, impaired discrimination or habituation of odors would not result in drastic life-threatening consequences in the affected dogs or *Ccdc66* -/- mice.

Besides the initially identified mutation in Schapendoes dogs and in the artificially generated *Ccdc66* -/- mouse, in humans, a disease causing mutation of the *CCDC66* gene has not yet been described. In a cohort of 80 RP and 20 Leber congenital amaurosis patients no pathogenic variant has been found (Gerding et al., 2011). In addition, a homozygous missense mutation in the *CCDC66* gene was recently excluded by linkage and segregation analysis to be disease causing in two Arabian siblings with retinal dystrophy, or in this particular type of retinal degeneration (Khan et al., 2018). The more precise description of the *Ccdc66* -/- mouse may allow to predict defined groups of patients with retinal degeneration of unknown cause (besides RP) that might be promising candidates to be tested for *CCDC66* mutation in order to identify disease-causing mutations in humans.

Database information on the pathogenetic relevance of *CCDC66* mutations is insufficient up to now (for example see NCBI or ExAC Browser). Next generation sequencing results barely classify/categorize *CCDC66* mutations. Since *CCDC66* might only be considered to have clinical relevance in retinal degenerations, probably exome analysis in cohorts of multisystemic diseases did not take into account *CCDC66* as potentially disease related gene.

In conclusion, the mutation localization within the *CCDC66* gene might be important regarding whether a mutation is disease causing or not; *CCDC66* RNA shows a complex splicing pattern. Depending on the location, not all CCDC66 protein isoforms might be affected by certain mutations and compensatory mechanisms might inhibit phenotypic manifestations. For example, *Ccdc66* RNA localization by *in situ* hybridization revealed clear expression in the WT retina, while it was almost absent in the *Ccdc66*-deficient mouse retina. On brain tissue slices, the pattern of *Ccdc66* RNA *in situ* hybridization does not obviously differ, comparing both genotypes (data not shown). Nevertheless, the fulllength CCDC66 isoform is lacking in the *Ccdc66*-deficient mouse as shown by Western blot analysis (Fig. 1A) and progressive effects of the trapped *Ccdc66* gene on olfactory structure and behavior are not negated by certain isoforms probably being still present. However, since in addition to the retinal phenotype, *Ccdc66*-deficient mice exhibit olfactory bulb degeneration along with olfactory impairment, the *Ccdc66* -/- mouse model adds the possibility to study mechanisms of central nervous system degeneration. Furthermore, the more precise description of the *Ccdc66*-deficient mouse phenotype presented here gives rise to the new categorization of the *Ccdc66* -/- mouse as a syndromic retinal disease model, supports a cilia-associated function of CCDC66 and suggests scrutinizing a broader spectrum of symptoms in human disease with possible contribution of *CCDC66* mutations.

Authors' contributions

SS wrote the manuscript with input from all authors. Light and electron microscopy was performed by EPP. Western blot experiments, X-gal staining were performed by SS supported by EP-K and WMG. The habituation/dishabituation test was performed by SS supported by EP-K and WMG. SS, EPP and EF contributed to the design and implementation of the research. JTE and WMG planned and coordinated the study. All authors discussed the results and contributed to the final manuscript and approved the final version.

Funding

This study was supported by German Research Foundation Grant DFG (EP 7/17 - 1) to JTE and the FORUM grant AZ F789-2013 from the Medical Faculty of the Ruhr-University Bochum to WMG.

Ethics approval

The authors certify that the experimental procedures were carried out in accordance with the European Communities Council Directive of 24 November 1986 (86/609/EEC) and with the German guidelines for animal care approved by the regional authority (LANUV, North-Rhine Westphalia, Germany; reference number 84-02.04.2015.A250).

Availability of data and materials

The datasets used and/or analyzed during the current study are available from the corresponding author on reasonable request.

Competing interests

The authors declare that they have no competing interests.

Acknowledgements

The excellent technical assistance of Marlen Löbbecke-Schumacher, Hans-Werner Habbes and Luzie Augustinowski as well as the great editing support of Cristina Gonzales-Liencres are gratefully acknowledged.

References

Baehr, W., Frederick, J.M., 2009. Naturally occurring animal models with outer retina phenotypes. Vision Res. 49, 2636–2652.

Blanchart, A., Romaguera, M., Garcia-Verdugo, J.M., de Carlos, J.A., López-Mascaraque, L., 2008. Synaptogenesis in the mouse olfactory bulb during glomerulus development. Eur. J. Neurosci. 27, 2838–2846.

Brinton, R., 2012. Minireview: translational animal models of human menopause: challenges and emerging opportunities. Endocrinology 153, 3571–3578. https://doi.org/10.1210/en.2012-1340.

Conkar, D., Culfa, E., Odabasi, E., Rauniyar, N., Yates 3rd, J.R., Firat-Karalar, E.N., 2017. The centriolar satellite protein CCDC66 interacts with CEP290 and functions in cilium formation and trafficking. J. Cell. Sci. 130, 1450–1462.

Curtis, M.A., Kam, M., Nannmark, U., Anderson, M.F., Axell, M.Z., Wikkelso, C., Holtas, S., van Roon-Mom, W.M., et al., 2007. Human neuroblasts migrate to the olfactory bulb via a lateral ventricular extension. Science 315, 1243–1249.

Dalke, C., Graw, J., 2005. Mouse mutants as models for congenital retinal disorders. Exp. Eye Res. 81, 503–512.

Dekomien, G., Vollrath, C., Petrasch-Parwez, E., Boevé, M.H., Akkad, D.A., Gerding, W.M., Epplen, J.T., 2010. Progressive retinal atrophy in Schapendoes dogs: mutation of the newly identified CCDC66 gene. Neurogenetics 11, 163–174.

Dias, M.F., Joo, K., Kemp, J.A., Fialho, S.L., da, Silva, Cunha, A., Jr, Woo, S.J., Kwon, Y.J., 2017. Molecular genetics and emerging therapies for retinitis pigmentosa: basic research and clinical perspectives. Prog. Retin. Eye Res. (17), 30052–30056. https://doi.org/10.1016/j.preteyeres.2017.10.004. Oct 31. pii: S1350-9462.

Doty, R.L., 2012. Olfactory dysfunction in Parkinson disease. Nat. Rev. Neurol. 8, 329–339 Review.

Dryja, T., McGee, T.L., Hahn, L.B., Cowley, G.S., Olsson, J.E., Reichel, E., Sandberg, M.A., Berson, E.L., 1990. Mutations within the Rhodopsin Gene in Patients with autosomal dominant retinitis pigmentosa. N. Engl. J. Med. 323, 1302–1307.

Gerding, W.M., Schreiber, S., Schulte-Middelmann, T., de Castro Marques, A., Atorf, J.,

Akkad, D.A., Dekomien, G., Kremers, J., et al., 2011. Ccdc66 null mutation causes retinal degeneration and dysfunction. Hum. Mol. Genet. 20, 3620–3631.
Graziadei, G.A., Graziadei, P.P., 1979. Neurogenesis and neuron regeneration in the olfactory system of mammals. II. Degeneration and reconstitution of the olfactory sensory neurons after axotomy. J. Neurocytol. 8, 197–213.
Hinds, J.W., Hinds, P.L., McNelly, N.A., 1984. An autoradiographic study of the mouse olfactory epithelium: evidence for long-lived receptors. Anat. Rec. 210, 375–383.
Kang, N., Baum, M.J., Cherry, J.A., 2009. A direct main olfactory bulb projection to the 'vomeronasal' amygdala in female mice selectively responds to volatile pheromones from males. Eur. J. Neurosci. 29, 624–634.
Khan, A.O., Budde, B.S., Nürnberg, P., Kawalia, A., Lenzner, S., Bolz, H.J., 2018. Genome-wide linkage and sequence analysis challenge CCDC66 as a human retinal dystrophy candidate gene and support a distinct NMNAT1-related fundus phenotype. Clin. Genet. 93, 149–154.
Kondo, K., Suzukawa, K., Sakamoto, T., Watanabe, K., Kanaya, K., Ushio, M., Yamaguchi, T., Nibu, K., et al., 2010. Age-related changes in cell dynamics of the postnatal mouse olfactory neuroepithelium: cell proliferation, neuronal differentiation, and cell death. J. Comp. Neurol. 518, 1962–1975.
Kornack, D.R., Rakic, P., 2001. Cell proliferation without neurogenesis in adult primate neocortex. Science 294, 2127–2130.
Lehmkuhl, A.M., Dirr, E.R., Fleming, S.M., 2014. Olfactory assays for mouse models of neurodegenerative disease. J. Vis. Exp. 90, e51804.
Lois, C., Alvarez-BuyIIa, A., 1994. Long-distance neuronal migration in the adult mammalian brain. Science 264, 1145–1148.
Mackay-Sim, A., Kitte, P.W., 1991. On the life span of olfactory receptor neurons. Eur. J. Neurosci. 3, 209–215.
Mockel, A., Perdomo, Y., Stutzman, F., Letsch, J., Marion, V., Dolifus, H., 2011. Retinal dystrophy in Bardet-Biedl syndrome and related syndromic ciliopathies. Prog. Retin. Eye Res. 30, 258–274.
Mori, K., Takahashi, Y.K., Igarashi, K.M., Yamaguchi, M., 2006. Maps of odorant molecular features in the mammalian olfactory bulb. Physiol. Rev. 86, 409–433.
Nuber, S., Petrasch-Parwez, E., Winner, B., Winkler, J., von Hörsten, S., Schmidt, T., Boy, J., Kuhn, M., et al., 2008. Neurodegeneration and motor dysfunction in a conditional model of parkinson's disease. J. Neurosci. 28, 2471–2484.
Petrasch-Parwez, E., Nguyen, H.P., Löbbecke-Schumacher, M., Habbes, H.-W., Wieczorek, S., Riess, O., Andres, K.H., Dermietzel, R., et al., 2007. Cellular and subcellular localization of Huntingtin [corrected] aggregates in the brain of a rat transgenic for Huntington disease. J. Comp. Neurol. 501, 716–730.
Pomeroy, S., LaMantia, A.-S., Purves, D., 1990. Postnatal construction of neural circuitry in mouse olfactory bulb. J. Neurosci. 10, 1952–1966 10.1523.
Roddick, K.M., Roberts, A.D., Schellinck, H.M., Brown, R.E., 2016. Sex and genotype differences in odor detection in the 3×Tg-AD and 5XFAD mouse models of Alzheimer's disease at 6 months of age. Chem. Senses 41, 433–440.
Rosenfeld, P.J., Cowley, G.S., McGee, T.L., Sandberg, M.A., Berson, E.L., Dryja, T.P., 1992. A null mutation in the rhodopsin gene causes rod photoreceptor dysfunction and autosomal recessive retinitis pigmentosa. Nat. Genet. 11, 209–213.
Sakano, H., 2010. Neural map formation in the mouse olfactory system. Neuron 67, 530–542.
Sarkar, S., Raymick, J., Imam, S., 2016. Neuroprotective and therapeutic strategies against Parkinson's disease: recent perspectives. Int. J. Mol. Sci. 17 pii: E904.
Schindelin, J., Rueden, C.T., Hiner, M.C., Eliceiri, K.W., 2015. The ImageJ ecosystem: an open platform for biomedical image analysis. Mol. Reprod. Dev. 82, 518–529.
Schwahn, U., Lenzner, S., Dong, J., Feil, S., Hinzmann, B., van Dujinhoven, G., Kirschner, R., Hemberger, M., et al., 1998. Positional cloning of the gene for X-linked retinitis pigmentosa 2. Nat. Genet. 19, 327–332.
Sharp, J.A., Plant, J.J., Ohsumi, T.K., Borowsky, M., Blower, M.D., 2011. Functional analysis of the microtubule-interacting transcriptome. Mol. Biol. Cell 22, 4312–4323.
Treloar, H.B., Miller, A.M., Ray, A., Geer, C.A., 2010. Development of the olfactory system. In: Menini, A. (Ed.), The Neurobiology of Olfaction. CRC Press/Taylor & Francis, Boca Raton (FL) Chapter 5.
Turmaine, M., Raza, A., Mahal, A., Mangiarini, L., Bates, G.P., Davies, S.W., 2000. Nonapoptotic neurodegeneration in a transgenic mouse model of Huntington's disease. Natl. Acad. Sci. U. S. A. 97, 8093–8097.
Wilson, K.C., Raisman, G., 1980. Age-related changes in the neurosensory epithelium of the mouse vomeronasal organ: extended period of postnatal growth in size and evidence for rapid cell turnover in the adult. Brain Res. 185, 103–113.
Yan, D., Liu, X.Z., 2010. Genetics and pathological mechanisms of Usher syndrome. J. Hum. Genet. 55, 327–335.
Yang, M., Crawley, J.N., 2009. Simple behavioral assessment of mouse olfaction. Curr. Protoc. Neurosci Chapter 8: Unit 8.24.
Young, R.W., 1967. The renewal of photoreceptor cell outer segments. J. Cell Biol. 33, 61–72.